Hindawi
International Journal of Rotating Machinery
Volume 2019, Article ID 9546831, 12 pages
https://doi.org/10.1155/2019/9546831

Research Article

Design and Production of Innovative Turbomachinery Components via Topology Optimization and Additive Manufacturing

Enrico Meli,[1] **Andrea Rindi**,[1] **Alessandro Ridolfi**,[1] **Rocco Furferi**,[1] **Francesco Buonamici**,[1] **Giuseppe Iurisci**,[2] **Simone Corbò**,[2] **and Francesco Cangioli**[2]

[1]*Department of Industrial Engineering, University of Florence, Via di S. Marta 3, 50139 Florence, Italy*
[2]*BHGE Nuovo Pignone, Via F. Matteucci 2, 50100 Florence, Italy*

Correspondence should be addressed to Enrico Meli; enrico.meli@unifi.it

Received 9 May 2019; Revised 18 July 2019; Accepted 25 July 2019; Published 2 September 2019

Academic Editor: Ryoichi Samuel Amano

The present paper proposes a methodology to design and manufacture optimized turbomachinery components by leveraging the potential of Topology Optimization (TO) and Additive Manufacturing (AM). The method envisages the use of TO to define the best configuration of the rotoric components in terms of both static and dynamic behavior with a resultant reduction of overall weight. Eventually, the topology-optimized component is manufactured by using appropriate materials that can guarantee valid mechanical performances. The proposed strategy has been applied to a 2D impeller used for centrifugal compressors to prove the effectiveness of a TO+AM-based approach. Although this approach has never been extensively used before to centrifugal compressors and expanders, its application on rotor and stator components might unlock several benefits: tuning the natural frequencies, a reduction in the stress level, and a lighter weight of the rotating part. These objectives can be reached alone or in combination, performing a single analysis or a multiple analyses optimization. Finally, the introduction of AM technologies as standard manufacturing resources could bring sensible benefits with respect to the time to production and availability of components. Such aspects are essential in the Oil and Gas context, when dealing with new projects but also for service operations.

1. Introduction

The increasing requirement for energy demands for highly efficient turbomachinery systems [1]. Consequently, Oil & Gas companies are nowadays facing major technological changes to increase the performances of their mechanical components and their overall competitiveness. Advanced design and manufacturing tools play a major role in costs reduction and in the development of a fast and efficient approach to the fabrication of advanced components. When dealing with rotoric components, the main challenge today is to move from traditional subtractive manufacturing to more flexible processes like, for instance, Additive Manufacturing (AM) [2]. The adoption of AM technologies for the fabrication of turbomachinery components could maximize the use of single-piece full milling machining thus reducing the need of welding/brazing joints. Indeed, several complications arise when dealing with jointing systems, the most important being the requirement of dedicated heat treatments. Such processes are not suitable for all the ranges of materials and, most importantly, can induce defects and geometrical distortions to the final piece.

CNC milling is the current golden standard for the manufacturing of single-piece impellers as it is able of reliably fabricating complex shapes (see Figure 1). On the other hand, CNC milling of impellers entails severe costs ascribable to (i) the need for high-end machines and utensils; (ii) long machining operations required to contour complex surfaces from raw material; (iii) waste of good material that is removed from the raw part in large amount. Summing up, the production of these pieces is generally slow and energetic; moreover, due to the complexity of the shapes that need to be manufactured (i.e. hollow objects with multiple undercuts),

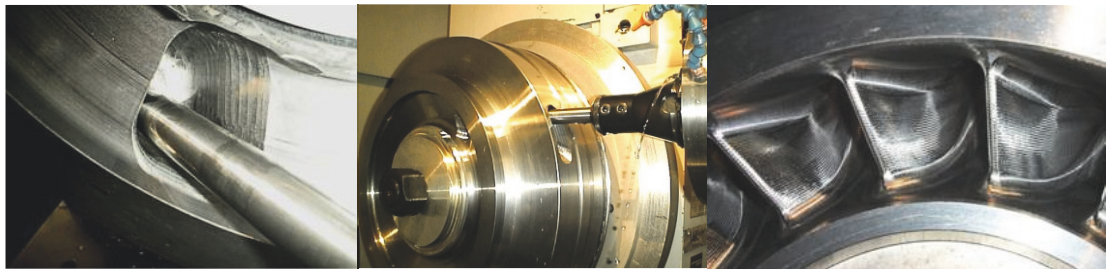

Figure 1: Some examples of impeller milling processes.

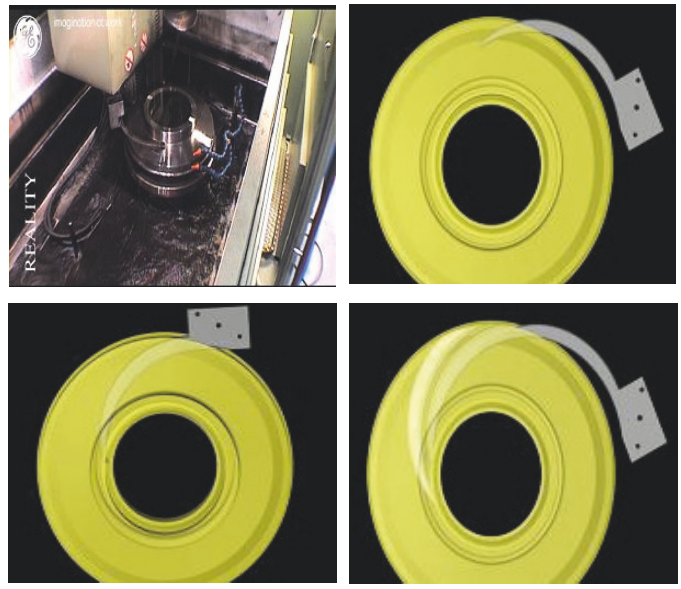

Figure 2: Impeller EDM operations.

each process is not trivial and needs to be carefully studied and designed [3].

When dealing with impellers characterized by narrow passage and simple flow passage, an elective process is the Electrical Discharge Machining (EDM). This method (see Figure 2) is extensively used since it is well suited for the production of very low flow coefficient impellers and it assures a high surface quality. On the other hand, EDM poses some limits for the fabrication of complex shapes and is time expensive.

It is important to highlight that the evolution of high-efficiency rotors has brought towards lighter structures that need to sustain higher speeds. Indeed, traditional subtractive technologies are less suited for the fabrication of slender structures, as the removal of higher volumes of materials is required. Additionally, modern design software allows shape optimizations in a relative short time, leading to complex geometries unconstrained from conventional mathematical surfaces. In this context, Topology Optimization (TO) software systems are among the most used design tools. Thanks to advanced optimization algorithms, they are able to improve the material distribution within a given design space for a given set of loads and boundary conditions such that the resulting layout meets a prescribed set of performance [4]. Accordingly, TO provides to the designer a great freedom, allowing complex structures, not immediately imaginable with traditional design methodologies [5].

Consequently, the adoption of AM for the fabrication of TO-produced designed usually represents a convenient choice because of the complexity of the shapes, which are produced with minimum attention at fabrication constraints. AM offers also significant advantages due to its short lead times and great geometrical freedom. This advantage makes AM the natural prosecution of TO processes [5, 6].

Dealing with the fabrication of impellers, the interest is directed to metal-based processes. In the last 5 years, metal AM process has seen great improvement in terms of mechanical performances of the parts produced and reliability and predictability of the process. As a result, metal AM processes are now an established alternative to traditional subtractive ones even for the fabrication of mechanical parts that need to sustain significant structural loads. According to [7] AM for Oil and Gas applications is in its beginning stages. Consequently, there is a limited scientific literature dealing with the complete design and manufacturing of turbomachinery components using AM, while a large number of works are focused on available metal additive manufacturing techniques and materials [8]. Metallurgical aspects of several

materials, such as for instance super-alloys, have been also investigated to understand the possibilities offered by AM in the turbomachinery sector [9]. Other works in literature deal with smart solutions for a wide range of applications including wear of diesel engine exhaust valves [10], corrosion of gas turbine blades [11], reparation of mold steels [12], wear of tools made of high-speed steel [13], and many others in which the conventional methods fail.

In [14] a first pilot study to apply both Topology Optimization and Additive Manufacturing for rotoric components has been carried out. In particular, a design method was applied to a turbine disk to obtain a safe range, without resonance conditions, around the frequency of the external loads and to reduce the weight. Beyond such pilot cases, to the best of authors' knowledge, this work is among the first ones dealing with a complete design of a TO/AM rotoric part.

Based on the above-mentioned considerations, the present paper proposes a unified approach for designing and manufacturing optimized turbomachinery components by leveraging the potential of Topology Optimization (TO) and Additive Manufacturing (AM). The method envisages the use of TO for defining the best configuration of the rotoric component in terms of both static and dynamic behavior with a resultant reduction of overall weight. Eventually, the topology-optimized component has been fully manufactured (both in Aluminum and in high resistance alloy like IN718) by using appropriate materials that can guarantee valid mechanical performances.

Specifically, the 3D printer technologies considered in this work are based on sintering through laser beam or electron beam; both processes are expensive and characterized by high-energy consumption. Moreover, final parts have surfaces with high porosity and surface roughness when compared with the ones obtained using traditional milling. Accordingly, postprocessing operations are usually required to obtain the desired quality. On the other hand, the possibility of manufacturing optimized parts with better performances in terms of static and dynamic behavior and lower weight encourages the effort to push forward AM in the turbocharger sector.

Even if the methodology is fully general, to prove the effectiveness of the proposed TO+AM approach, a specific high pressure impeller of a centrifugal compressor has been chosen as test case in this paper due to the critical characteristics of this application in terms of geometry and working conditions.

Finally, it is noteworthy that the approach presented in this paper, if extensively applied to rotating turbomachinery components, might unlock several benefits: tuning the natural frequencies, a reduction in the stress level, and a lighter weight of the rotating part, thus enabling higher speeds and improvement of thermodynamic performances. The design of structurally efficient shapes can lead, in turn, to a weight reduction of the parts, with a consequent abatement of costs.

2. Materials and Methods

As mentioned above, the present work aims to describe a method for designing optimized rotoric components used for Oil & Gas sector (e.g. turbine disks or impellers) and for additive manufacturing of them. Some constraints, detailed in the text to follow, are taken into account with the aim of manufacturing efficient impellers:

(i) the material used for the component that should guarantee the following properties: high ductility at different operating temperature (that can go from cryogenic up to 400°C);

(ii) corrosion resistance induced by the presence of water and CO_2 and in presence of H_2S;

(iii) pitting resistance induced by the presence of chlorides;

(iv) high strength to sustain the working condition (pressure and speed);

(v) market availability of the material, in order to keep low supply times and cost.

Therefore, the proposed design method is based on the following steps (Figure 3) which envisage design, material selection, and manufacturing of the component:

(i) Step 1: test case definition and characterization; in the present work, the selected case is a 2D impeller used in centrifugal compressors. The choice of a test case allows understanding the steps to perform the design procedure. Nonetheless, the same approach can be applied on a wide range of rotoric components.

(ii) Step 2: definition of the design space for the optimization procedure. Such a design space consists on an extended area whose geometry can be dramatically changed during the topology optimization routine.

(iii) Step 3: definition of an appropriate objective function (OF) to be minimized during optimization. Together with the definition of the desired OF, also optimization constraints for both static and dynamic characteristics (i.e., natural frequencies, stress, manufacturing, and volume fraction) are here defined.

(iv) Step 4: static and modal TO.

(v) Step 5: materials selection and AM of the component.

The overall process and the tools used to perform each step will be described with reference to a specific test case (i.e., a centrifugal compressor impeller, detailed in the text to follow) in order to present the method with a practical approach. As a result, test-case specific information (design specifications, constraints, and geometry) is provided in each step to discuss the application of the procedure. Whereas specific aspects of the chosen test case are provided throughout the entire manuscript, the intent is to provide the reader with a general comprehension of the method.

Step 1 (test case definition and characterization). Compressors are the parts of an engine responsible for providing enough air with enough pressure to the combustion chamber. In most cases, gas turbine engines have two compressors: low-pressure and high-pressure, which operate at different working temperatures. The low-pressure compressor usually

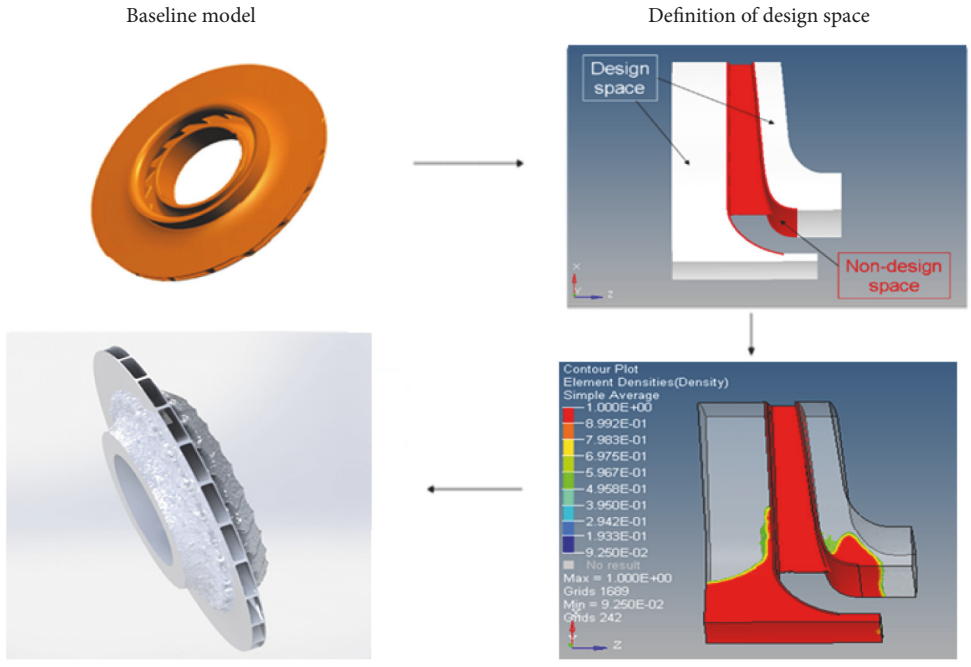

Figure 3: Framework of the proposed design method.

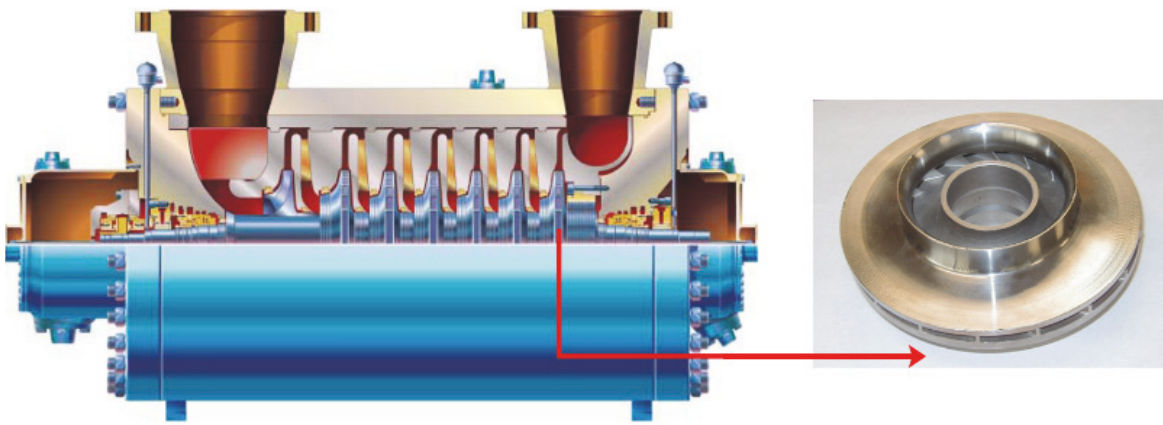

Figure 4: GE impeller used as a starting point for carrying out the novel design.

works at relatively low temperatures, around 350°C, whereas the high-pressure compressor works at temperatures in the range of 500°C to 600°C. Accordingly, the selected test case is a 2D impeller (i.e., an impeller characterized by two-dimensional blades in the radial part) used in centrifugal compressors [15]. In detail, a previously designed impeller used by GE is used as a starting point for the optimization procedure (see Figure 4). The main specifications of the selected impeller are reported in Table 1.

Moreover, the impeller is considered as composed by a material with linear elastic isotropic properties as listed in Table 2.

Table 1: Specification of analyzed stage.

Flow Coefficient	0.0444
Mach	0.73
Diameter [mm]	390
Vane number	*23*

Prior to optimizing the design of the selected case study, it is necessary to perform its complete characterization in terms of both static and modal behavior. This characterization, carried out by means of a Finite Element Analysis (FEA),

Table 2: Material Properties.

Young's Modulus (E)	$2.2*10^5$ MPa
Poisson's Ratio (ν)	0.3
Density (ρ)	$7.85*10^3$ kg/m3

Table 3: Maximum stress in the whole impeller and maximum radial displacement in the interference region between impeller and shaft.

Maximum stress [MPa]	561
Maximum displacement [mm]	0.14

provides the baseline for assessing the performance of topologically optimized design. In particular, the FEA allows to estimate both the maximum displacement and the maximum stress of the impeller (see Table 3).

The boundary conditions imposed during the FEA are as follows:

(i) Two nodes at impeller front hub constrained in the tangential direction.

(ii) Two nodes at impeller back hub constrained in the axial direction.

The only external load applied to the rotating component is a static loading condition due to a centrifugal force field (see Equation (5)). The rotational velocity is set to 14700 rpm (245 Hz) which is the speed at full capacity for this specific rotor. Symmetry of the entire part (23 identical vanes) allows for a simplified analysis performed only on a circular 15.65° sector of the part. Accordingly, cyclic symmetry constraints are used to analyze the whole impeller.

The distribution of von Mises stresses on the benchmark geometry is depicted in Figure 5. The maximum von Mises stress value results equal approximately 550 MPa. Beside some hot spots that are evidently generated by stress concentrations factors induced by the specific geometry of the rotoric component, it is possible to identify a general stress gradient that moves from the internal to the external radius that is coherent with the application.

The impeller was characterized also by means of a modal analysis since the main objective for the subsequent TO is to move away from the operating range particular vibrating modes (i.e., away from the frequency range near the working frequency $\omega_w = N * \omega = 5635$ Hz, where N is the number of vanes and ω is the machine speed). The natural modes of the test case impeller are reported in Table 4. The modes from 12 and 13 are dangerously near the operating range and should be kept outside it, with a margin of at least 150 Hz. At the same time, it is important not to bring additional modes inside the operating range, as the mode 10, 11 or 14, 15.

Step 2 (design space definition). When a generic TO has to be carried out, it is necessary to define the design space, i.e., an area enclosing the set of elements that can be changed during the optimization. Oppositely, the nondesign space defines model regions that remain unchanged during the optimization routine. Referring to the selected test case, the

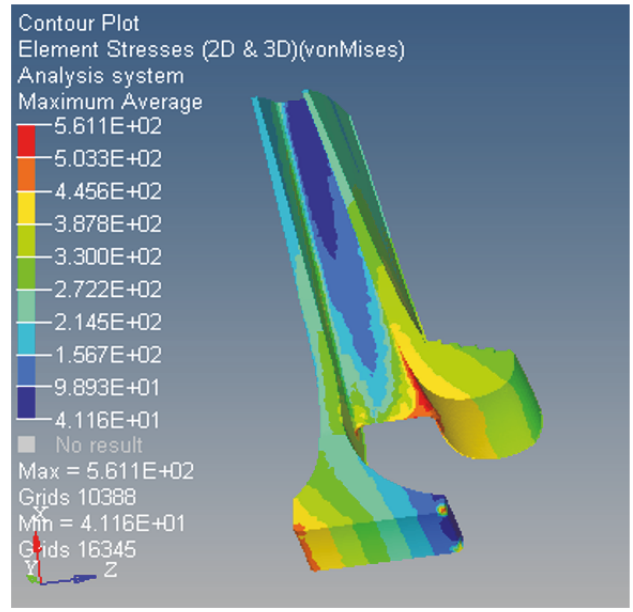

Figure 5: Stress distribution obtained by FEM on the benchmark geometry.

blade region must be preserved; accordingly, it belongs to the nondesign space. The analysis design space to be considered includes both hub and shroud regions. A graphical explanation of design and nondesign space is given in Figure 6. The white volumes represent the design space while the red ones are the nondesign space of the topological optimization.

Step 3 (objective function and optimization constraints). In the formulation of optimization problems, some quantities can be used as objective function to be minimized (usually global quantities) and some others as constraints (usually local quantities): compliance, natural frequencies, volume (or volume fraction), mass (or mass fraction), displacements, stresses, and strains.

The minimization of objective functions drives the seek for an optimized shape. Two main strategies have been tested in this work: minimizing the volume and minimizing the compliance. The minimization of the volume (see (1)) often causes convergence problems, which produce irregular final geometries:

$$V\left(\rho_f\right) = \int_\Omega \rho_f d\Omega \tag{1}$$

where ρ_f is the material density and Ω is the domain.

On the contrary, compliance minimization is very interesting and promising also according to literature studies [16]. Compliance $l(u)$ is defined as follows:

$$l\left(u\right) = \int_\Omega \underline{f}.\underline{v}d\Omega + \int_{\Gamma_T} \underline{t}.\underline{u}ds \tag{2}$$

where f are the body forces (centrifugal load in this work) on the domain Ω and t are the boundary tractions on the traction part $\Gamma_T \subset \partial\Omega$.

Table 4: Impeller natural modes.

Mode	1	2	3	4	5	6	7	8	9	10	11	12	13	14	15	16
Frequency (Hz)	33 00	33 01	38 32	38 33	44 92	48 54	48 55	49 66	49 67	50 27	50 28	56 63	56 64	58 82	58 83	63 61

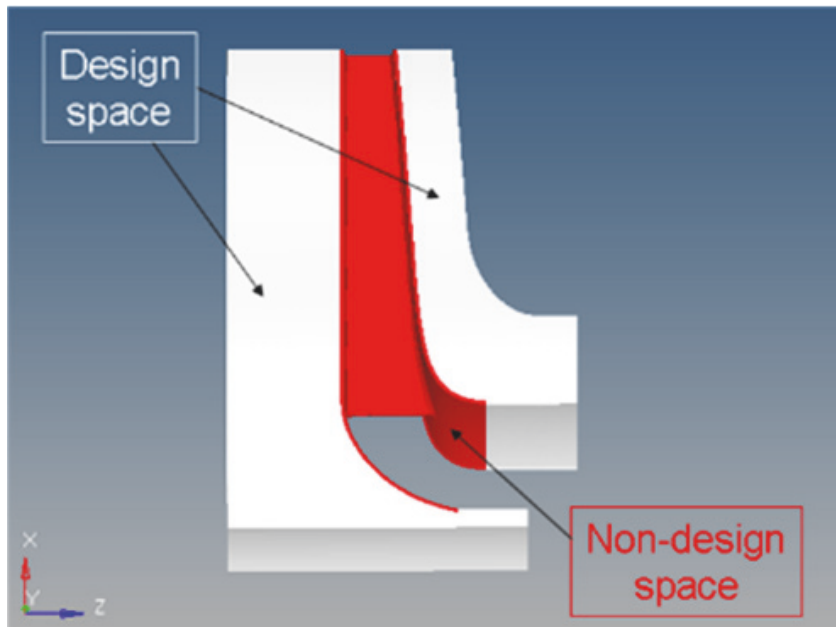

Figure 6: TO domain: design and nondesign space.

The compliance is the strain energy of the structure and it can be considered a reciprocal measure for the stiffness of the structure. It is defined for the whole structure, since the objective functions must be referred to a global parameter. The objective of the minimum compliance problem is to find the material density distribution that minimizes the structure deformation under the prescribed support (boundary conditions) and loading conditions.

The optimization constraints used in this work are on the displacements in the area of interference between the shaft and impeller (in order to avoid detachments), on the maximum value of the stress and on the volume fraction (see (3)). The volume fraction is defined as the ratio of the difference between the total volume at current iteration and the initial nondesign volume to the initial design volume. This constraint is applied to guarantee the permanence of a volume fraction in a specific part: in particular, analysing preliminary results, it has been decided to introduce this constraint to the outer disk, because the solver tends to completely remove this part.

The various constraints can be defined as follows:

$$\begin{aligned} \sigma_{max} &< \sigma_r \\ u_{max} &< u_r \\ V_{fr,min} &< V_{fr} \end{aligned} \tag{3}$$

where

(i) σ_{max} is the maximum allowable values of stress in the optimized model;

(ii) σ_r is the maximum values of stress, equal to or lower than the benchmark value, to be set in the optimization test;

(iii) u_{max} is the maximum interference area radial displacements allowable in the optimized model;

(iv) u_r is the maximum radial displacements to be set during the optimization test;

(v) $V_{fr,min}$ is the minimum volume fraction for the optimized model, introduced to avoid the whole part deletion by the solver;

(vi) V_{fr} is the minimum design volume fraction to be set in the topology optimization test.

Step 4 (static and modal topological optimization). In the proposed framework, the TO problem is carried out by using the Solid Isotropic Material with Penalization (SIMP) method [17, 18]. Through this density method, a pseudo material density ρ_f is used as the design variable. During the TO procedure, ρ_f of each element varies continuously between 0 and 1, defining the element as being, respectively, either completely void or solid. Intermediate values of density represent fictitious material. The SIMP method applies a power-law penalization for the relationship between stiffness and density in order to set density toward 0 and 1 (void and solid) distribution. The stiffness of the material is assumed

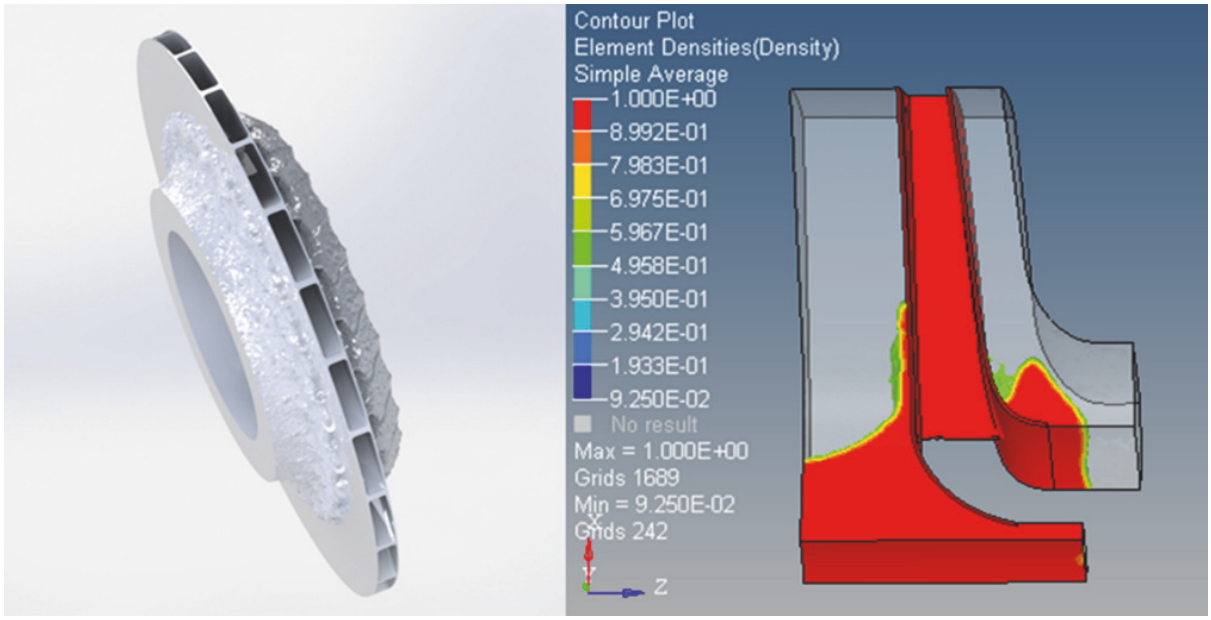

Figure 7: Optimization result for the 2D impeller.

linearly dependent on the density. In general, the optimal solution of problems involves large areas of intermediate densities in the structural domain. Techniques need to be introduced to penalize intermediate densities and to force the final design to be represented by densities of 0 or 1 for each element. The penalization technique used is the power law representation of elasticity properties, which can be expressed as follows:

$$E = E_0 \left[\rho^p\right] \tag{4}$$

where

(i) E is the optimum stiffness of the topology element;

(ii) E_0 represents the stiffness of the initial design space material;

(iii) p is the penalty factor applied to the density to control the generation of intermediate density elements (high, medium, and low porosity);

The constraints on stress, displacements, and volume, introduced in the previous step, are set as follows:

(i) σ max < 500 MPa;

(ii) u max < 0.100 mm;

(iii) V_{fr} min > 20 %, on the outer disk.

The centrifugal load acting on shroud, blade, and hub can be described as follows:

$$\underline{f}_{CF} = \rho\omega^2 \begin{pmatrix} x \\ y \\ 0 \end{pmatrix} \tag{5}$$

Table 5: 2D impeller optimization results.

	Baseline	Optimization	Reduction
Maximum stress [MPa]	561	408	27%
Maximum displacement [mm]	0.14	0.10	28%

where $\underline{f}_{CF}$ is the centrifugal load, ρ is the material density, and ω is the rotational speed (around the z axis).

Finally, a further set of constraints is imposed with the aim of performing modal optimization:

(i) mode 10, 11 frequency < 5475 Hz;

(ii) mode 12, 13 frequency > 5785 Hz.

The main objective of the modal constraints is to move away from the operating range particular vibrating modes (see Table 4 and the "Step 1" chapter). The modes from 12 and 13 are dangerously near the operating range and should be kept outside it, with a margin of at least 150 Hz. At the same time, it is important not to bring additional modes inside the operating range, as the mode 10, 11 or 14, 15.

The best performance for the static and modal topological optimization is reported in Figure 7 on the right (the rendered version of the optimized 2D impeller is reported on the left). Red regions are the unit density zones, while no results volumes are no density, respectively, no material volumes. The values of maximum stress and radial displacement are summarized in Table 5. Both von Mises maximum stress and maximum displacement have seen a significant reduction, thus confirming the optimized mechanical behavior of the newly designed impeller.

At this step of the research activity, the dynamical loads have been considered into the optimization procedure in terms of frequency constraints to keep the modal frequencies

Table 6: Baseline and optimized Impellers natural modes.

Mode	Baseline Freq. (Hz)	Optimized Freq. (Hz)
11	5028	5462
12	5663	5795

of the optimized system away from the "most probable" frequency operating range of the machines. At the same time, since the operating conditions of the machine at such frequency may be quite variable and different from the nominal one during the machine life, the authors did not apply a specific dynamical load in terms of harmonic pressure field on the blades of the compressors. This harmonic pressure field would be, indeed, related to a specific machine working condition, and not fully representative of the pressure loads acting on the machine during its entire life. However, during the next step of the research activities, numerical and experimental fluid dynamical analyses will be performed "a posteriori" to verify the performances of the optimized components under specific operating conditions.

The results in terms of modes are summarized in Table 6. All the constraints in terms of frequency and stress are respected and the overall mass of the impeller is reduced by almost 30%.

Furthermore, it has to be highlighted that the algorithm has removed mass at the zone at higher diameter, which is the area that vibrates more, reducing the stiffening of the structure. At the same time, to keep the stress level below 500 MPa, a series of reinforcement along the blade tip are created, together with a concentration of mass on the eye region, above the blade leading edge. These features are able to reduce the stiffness of the impeller by keeping at an acceptable level both blade deformations and stresses.

It is important to note that, in this phase of the research activity, the target is to perform the structural optimization of the component. In particular, the dependence of the material characteristics on the temperature (thermal expansion, Young modulus, etc.) has been considered, but the working temperature has been kept constant. In other words, a complete thermostructural optimization (involving the optimization of temperature and thermal flux, and computationally much heavier) has not been performed yet.

However, during the next step of the research activities, numerical and experimental thermal analyses will be performed "a posteriori" to verify the performances of the optimized components under specific operating conditions. Furthermore, a complete thermostructural optimization of analogous components and of components working at higher temperatures will be performed. For high temperature components, high resistance titanium alloys will be considered as well.

Step 5 (materials selection and AM of the component). As already mentioned, the optimized geometry of the impeller is not obtainable using traditional subtractive technologies and therefore the only viable way to manufacture it is to adopt AM. Since the desired model is not a mere mock-up of the impeller but rather a fully operating prototype, metal AM is the elective technology to produce such a part. Therefore, a preliminary analysis of most promising materials for turbomachinery applications was conducted. One of the most interesting materials investigated, is the IN718 [19], a precipitation hardenable nickel-based alloy characterized by exceptionally high yield, tensile and creep-rupture properties at temperatures up to 700°C. Such a material has been characterized in terms of both physical resistance (strength, ultimate tensile strength UTS, % elongation to rupture) and corrosion resistance (CO2, water, and H2S corrosion resistance), with dedicated test according to NACE recommendations [14].

In detail, using both direct metal laser sintering (DMLS) and traditional forging a number of specimens are produced. Then, such specimens are tested to compare their performance. For a design standpoint, a complete characterization of the materials has been performed exploring fatigue and tensile properties of the material, directly compared with the corresponding wrought alloy. A good matching of the characteristics is obtained after welding parameters set up phase finding that the DMLS specimen has a better ductile behavior, that is found in both higher elongation and lower UTS at lower temperature. Variability in the DMLS process is comparable to the forging one since the data statistically processed shows approximatively the same standard deviation for the two processes.

Furthermore, a metallographic examination has been carried out; Figure 8 shows a similar material grain size and disposition of the base material for additive manufactured specimen and forged one.

Moreover, corrosion resistance behavior is in line with wrought material. In conclusion, it is possible to prove that the 3D printed IN718 may be considered a very good alternative to forgings, at least for components sizes that are within printable dimensions, as also demonstrated by scientific literature [20].

After the material characterization has been carried out, showing the good mechanical properties of the selected alloy, it is possible to manufacture the optimized component. As already mentioned, the selected technology is the DMLS additive manufacturing. High-precision DMLS parts possess exceptional surface characteristics along with mechanical properties equivalent to those found in traditional wrought materials after that proper heat treatment is carried out [21]. Surface quality and minimal porosity are two key advantages of the DMLS process. It is important to note that, thanks to the ongoing development of AM technology, performances that can be obtained on various aspects are continuously improved. The research is especially active in the area of superalloys, which represent a class of materials particularly interesting for high-performance applications and oil & gas applications specifically. For example, fatigue behavior of IN718 AM structures is well documented in [22]. Similarly, oxidation resistance of IN718 is studied in [23], where a comparison between AM and forging is carried out. Finally, even FE analyses and simulations of the AM process have recently improved and are capable of providing reliable results. As an example, [24] addresses the problem of the

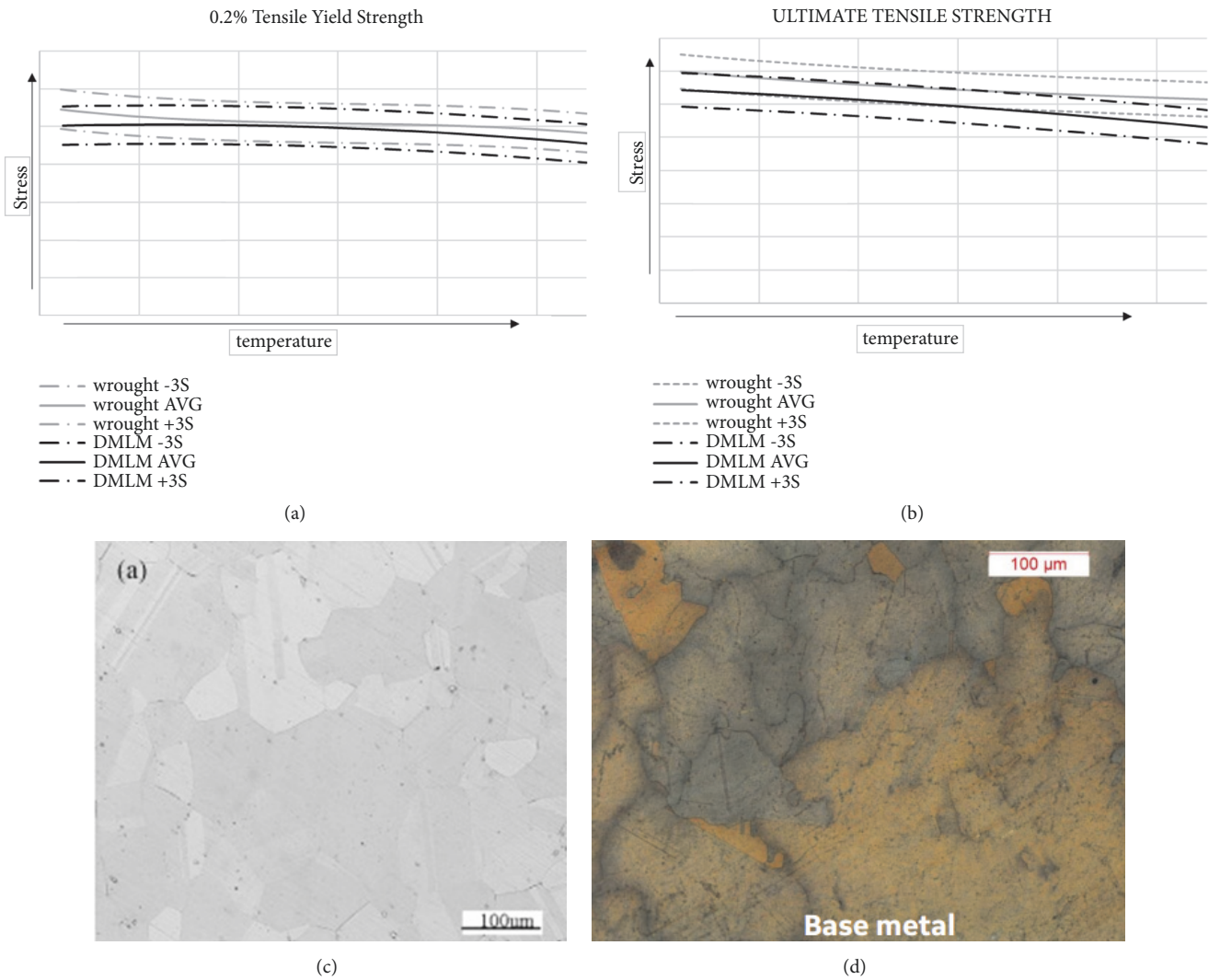

Figure 8: Metallographic examination results: (a) 0.2% tensile yield strength comparison; (b) UTS comparison; (c) wrought IN718 micrographic examination; (d) DMLS IN718 micrographic examination.

influence of process parameters of EBM-manufactured parts on the grain morphology of IN718 parts.

In detail, the machine adopted to create the prototypes is the EOS M400, with a volume capability of 400x400x400mm. Since the designed component is characterized by unusual geometries, also due to the very low flow coefficient (i.e., below 0.0100) which encompasses very narrow blade passages, prior to manufacture of the model using IN718 powder, a dummy model has been realized. The selected material to create such a model is aluminum. The steps followed to obtain the prototype are as follows:

(i) definition of the model position and orientation within the machine building volume. Such step should be carefully carried out in order to reduce the incidence of thermal deformations and residual stresses to the manufactured part. Moreover, even surface quality can be affected by the orientation of the part: this aspect should be taken into account to reduce the need for postprocessing operations.

(ii) deposition and melting of metal powder as per DMLS process, tuned to increase the geometrical quality of the dummy part;

(iii) heat treatment of the part produced to reduce deformation induced by the AM process;

(iv) removal of the internal support, needed to sustain overhang structures at angle above 45°;

(v) final machining to achieve the desired external geometry;

(vi) finishing process to reduce the final roughness in the flow path region.

The process parameters have been tuned according to the proprietary know-how of BHGE and studies available in literature (e.g., [25]). The optimized compressor impeller produced in Aluminum is shown in Figure 9.

To verify the effectiveness of the additive process to create the prototype, a number of dimensional measurements

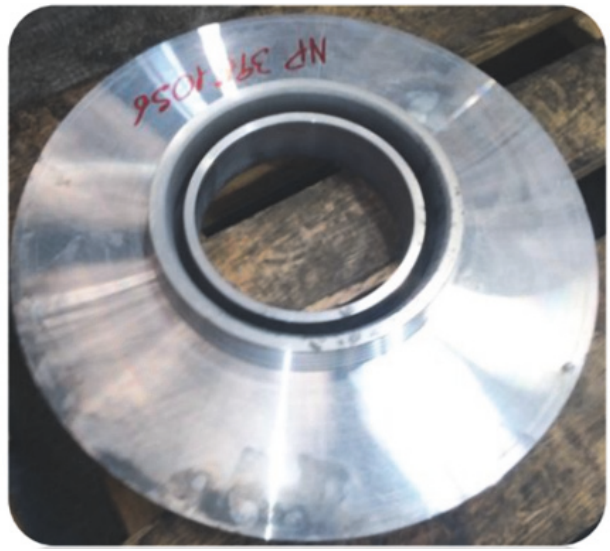

Figure 9: Optimized compressor impeller produced in Aluminum.

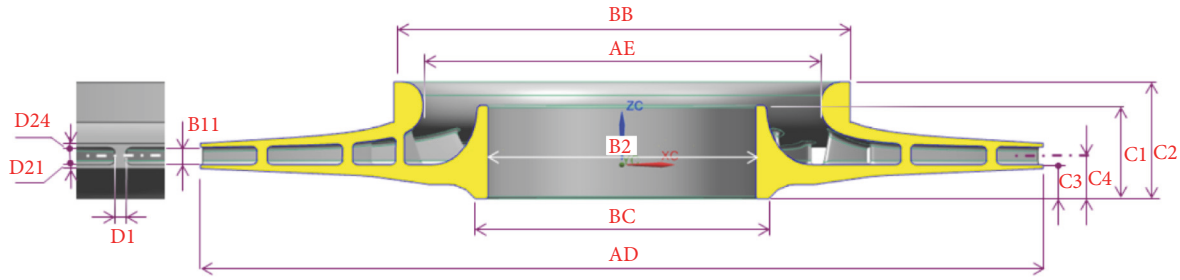

Figure 10: Dimension definition for geometrical control.

Table 7: Impeller dimensions outside requested tolerances.

Parameter	Description	Difference vs nominal
B3	Inner Diameter	-0.01%
C1	Foot length	2.27%
C2	Total length	1.38%
BB	Seal diameter	-0.03%
B11	average exit width	-3.86%
D21	Average Disk thickness at exit	11.11%
D24	Average Shroud thickness at exit	52.78%

were carried out to verify the compliance of the model with geometric dimensions, tolerances, and roughness. Measured dimensions are in Figure 10. The comparison between measured and expected data are in Table 7.

The final geometries were within the requested dimensional and geometrical tolerances, with a final roughness achieved through abrasion flow machining. The main differences are measured on the hub and shroud thickness at the exit region; however, it is possible to machine the external part to achieve the required dimensions.

Given for granted the good results obtained for the dummy Al model, the final step consisted in manufacturing the IN718 final prototype (see Figure 11). The same steps followed for the fabrication of the dummy prototype have been applied for the fabrication of the final prototype. Literature studies [26, 27] on the effect of the DMLS settings and on the positioning of the part have been taken into account to maximize the desired mechanical and geometrical properties.

3. Conclusions and Further Developments

Along this paper an introduction to innovative manufacturing process and related design approaches has been presented, highlighting the strength and the weakness of both and showing how the printing techniques shall be thought not just as an alternative to conventional processes but as a new technology enabling generating geometries that could not be imagined before. The results reported show how topological optimization gives promising results in terms of mass reduction and stress optimization dynamic response of the structure and that many design space constraints can be removed if coupled with additive manufacturing techniques. Significant improvements in terms of mechanical

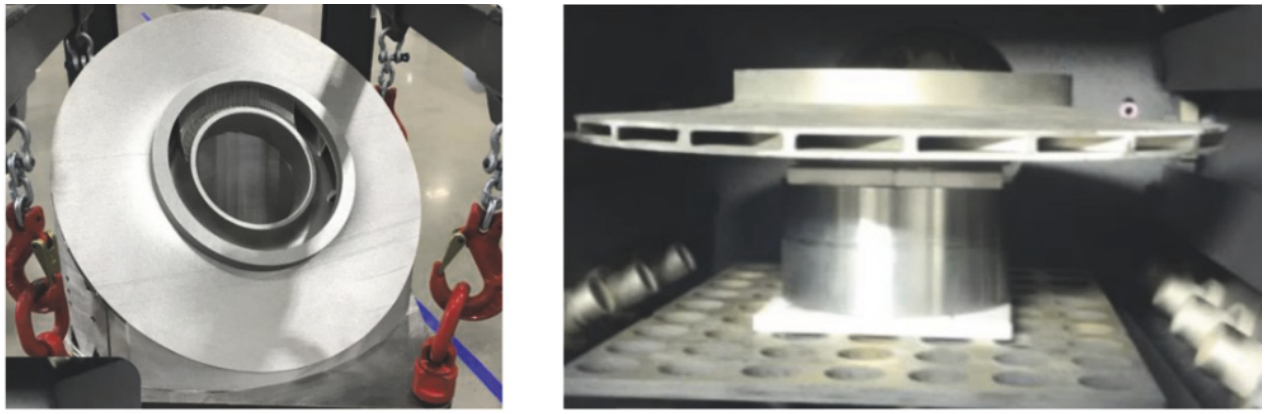

Figure 11: Final prototype of the impeller.

performance have been achieved: the stresses values and the radial displacements of the interference zone have been reduced if compared to traditional design, decreasing the impeller weight as well. The resulting structure is lighter and satisfies all design constraints. This aspect has allowed raising rotational velocity and then the machine efficiency.

The best configuration of constraints and objective functions to obtain new components structures was defined. The best strategy to obtain promising results is minimizing the total compliance, with constraints on local stress, displacement, and volume fractions. The "ready to print geometry" can be produced by a rendering process, after each optimization to create a smooth 3D model for the manufacturing.

Concerning the future developments of the research activity, numerical and experimental fluid dynamical analyses (in aluminum and IN718) will be performed to verify the mechanical characteristics of the optimized components under specific operating conditions [24] (both statically and dynamically). Numerical and experimental thermal analyses will be carried out on the optimized components as well. Furthermore, a complete thermostructural optimization of analogous components and of components working at higher temperatures will be performed. For high temperature components, high resistance titanium alloys will be taken into account as well. Finally, suitable post–AM thermal treatments and surface finishes/coatings will be considered to improve the mechanical properties of the impellers (especially in terms of fatigue resistance).

Overall, the main goal of the new research steps will be the optimization of the whole production process (structural optimization; additive manufacturing; post–AM treatments). To this end, new and more extreme structural optimization techniques (as, for example, lattice topology optimization) will be taken into account.

Data Availability

The data used to support the findings of this study are included within the article.

Conflicts of Interest

The authors declare that they have no conflicts of interest.

Acknowledgments

The authors would like to thank "BHGE, a GE Company" for the precious support during all the phases of the research activity and for providing the required technical documentation.

References

[1] X. Lei, M. Qi, H. Sun, and L. Hu, "Investigation on the Shock Control Using Grooved Surface in a Linear Turbine Nozzle," in *Proceedings of the ASME Turbo Expo 2017: Turbomachinery Technical Conference and Exposition*, p. V02CT44A021, Charlotte, North Carolina, USA, 2017.

[2] J. M. Justino Netto and Z. D. Silveira, "Design of an innovative three-dimensional print head based on twin-screw extrusion," *Journal of Mechanical Design*, vol. 140, no. 12, p. 125002, 2018.

[3] K. Chen, "Investigation of tool orientation for milling blade of impeller in five-axis machining," *The International Journal of Advanced Manufacturing Technology*, vol. 52, no. 1-4, pp. 235–244, 2011.

[4] H. Kazemi, A. Vaziri, and J. A. Norato, "Topology optimization of structures made of discrete geometric components with different materials," *Journal of Mechanical Design*, vol. 140, no. 11, p. 111401, 2018.

[5] M. E. Orme, M. Gschweitl, M. Ferrari, I. Madera, and F. Mouriaux, "Designing for additive manufacturing: lightweighting through topology optimization enables lunar spacecraft," *Journal of Mechanical Design*, vol. 139, no. 10, p. 100905, 2017.

[6] E. Ulu, R. Huang, L. B. Kara, and K. S. Whitefoot, "Concurrent structure and process optimization for minimum cost metal additive manufacturing," *Journal of Mechanical Design*, vol. 141, no. 6, p. 061701, 2019.

[7] G. Fayaz and S. Kazemzadeh, "Towards additive manufacturing of compressor impellers: 3D modeling of multilayer laser solid freeform fabrication of nickel alloy 625 powder mixed with nano-CeO2 on AISI 4140," *Additive Manufacturing*, vol. 20, pp. 182–188, 2018.

[8] A. W. Gebisa and H. G. Lemu, "Additive manufacturing for the manufacture of gas turbine engine components: literature review and future perspectives," in *Proceedings of the ASME Turbo Expo 2018: Turbomachinery Technical Conference and Exposition*, p. V006T24A021, Oslo, Norway.

[9] C. Boig, M. Burkinshaw, and I. Todd, *The Application of Additive Manufacturing to Turbomachinery*, 2018.

[10] C. Navas, A. Conde, M. Cadenas, and J. De Damborenea, "Tribological properties of laser clad Stellite 6 coatings on steel substrates," *Surface Engineering*, vol. 22, no. 1, pp. 26–34, 2006.

[11] H. Wang, D. Zuo, X. Li, K. Chen, and M. Huang, "Effects of CeO2 nanoparticles on microstructure and properties of laser cladded NiCoCrAlY coatings," *Journal of Rare Earths*, vol. 28, no. 2, pp. 246–250, 2010.

[12] C. Navas, A. Conde, B. Fernández, F. Zubiri, and J. de Damborenea, "Laser coatings to improve wear resistance of mould steel," *Surface and Coatings Technology*, vol. 194, no. 1, pp. 136–142, 2005.

[13] W. Darmawan, J. Quesada, F. Rossi, R. Marchal, F. Machi, and H. Usuki, "Improvement in wear characteristics of the AISI M2 by laser cladding and melting," *Journal of Laser Applications*, vol. 21, no. 4, pp. 176–182, 2009.

[14] "Corrosion Basics - NACE n.d," https://www.nace.org/resources/general-resources/corrosion-basics, 2019.

[15] Y. Galerkin, A. Reksrin, and A. Drozdov, "2D and 3D impellers of centrifugal compressors – advantages, shortcomings and fields of application," *IOP Conference Series: Materials Science and Engineering*, vol. 232, p. 012040, 2017.

[16] S. Wang, K. Lim, B. Khoo, and M. Wang, "An extended level set method for shape and topology optimization," *Journal of Computational Physics*, vol. 221, no. 1, pp. 395–421, 2007.

[17] M. P. Bendsøe, "Optimal shape design as a material distribution problem," *Journal of Structural Optimization*, vol. 1, no. 4, pp. 193–202, 1989.

[18] A. Rindi, E. Meli, E. Boccini, G. Iurisci, S. Corbò, and S. Falomi, "Static and modal topology optimization of turbomachinery components," *Journal of Engineering for Gas Turbines and Power*, vol. 138, no. 11, Article ID 112602, 2016.

[19] "INCONEL ® alloy 718. n.d".

[20] L. Murr, "Metallurgy of additive manufacturing: Examples from electron beam melting," *Additive Manufacturing*, vol. 5, pp. 40–53, 2015.

[21] B. Dutta and F. H. Froes, "The Additive Manufacturing (AM) of titanium alloys," *Metal Powder Report*, vol. 72, no. 2, pp. 96–106, 2017.

[22] L. Huynh, J. Rotella, and M. D. Sangid, "Fatigue behavior of IN718 microtrusses produced via additive manufacturing," *Materials & Design*, vol. 105, pp. 278–289, 2016.

[23] C. Juillet, A. Oudriss, J. Balmain, X. Feaugas, and F. Pedraza, "Characterization and oxidation resistance of additive manufactured and forged IN718 Ni-based superalloys," *Corrosion Science*, vol. 142, pp. 266–276, 2018.

[24] N. Raghavan, R. Dehoff, S. Pannala et al., "Numerical modeling of heat-transfer and the influence of process parameters on tailoring the grain morphology of IN718 in electron beam additive manufacturing," *Acta Materialia*, vol. 112, pp. 303–314, 2016.

[25] F. Calignano, D. Manfredi, E. P. Ambrosio, L. Iuliano, and P. Fino, "Influence of process parameters on surface roughness of aluminum parts produced by DMLS," *The International Journal of Advanced Manufacturing Technology*, vol. 67, no. 9-12, pp. 2743–2751, 2013.

[26] P. F. Kelley, A. Saigal, J. K. Vlahakis, and A. Carter, "Tensile and Fatigue Behavior of Direct Metal Laser Sintered (DMLS) Inconel 718," in *Proceedings of the ASME 2015 International Mechanical Engineering Congress and Exposition*, vol. 2A Advanced Manufacturing, p. V02AT02A001, Houston, Texas, USA, 2015.

[27] Q. Shi, D. Gu, M. Xia, S. Cao, and T. Rong, "Effects of laser processing parameters on thermal behavior and melting/solidification mechanism during selective laser melting of TiC/Inconel 718 composites," *Optics & Laser Technology*, vol. 84, pp. 9–22, 2016.